Int J Legal Med (2002) 116 : 5–11

ORIGINAL ARTICLE

G. Bocaz-Beneventi · F. Tagliaro · F. Bortolotti
G. Manetto · J. Havel

Capillary zone electrophoresis and artificial neural networks for estimation of the post-mortem interval (PMI) using electrolytes measurements in human vitreous humour

Received: 23 January 2001 / Accepted: 29 May 2001

Abstract Determination of electrolyte concentrations (mainly potassium) in vitreous humour has long been considered an important tool in human death investigations for the estimation of the post-mortem interval (PMI). On the basis of its well known potential in ion analysis, capillary zone electrophoresis (CZE) has recently been applied to achieve a rapid and simultaneous determination of inorganic ions in this extracellular fluid. In the present work, artificial neural networks (ANN) were applied for modelling of the relationship of multicomponent CZE analysis of K^+, NH_4^+, Na^+, and Ba^{2+} ions in vitreous humour with PMI. In a study based on 61 cases with different causes of death and a known PMI ranging from 3 to 144 h, the use of ANNs considering all inorganic ion data from the human vitreous humour, achieved a substantial improvement of post-mortem interval prediction. Good linear correlation was observed ($r^2 = 0.98$) and in comparison to the traditional linear least squares (LLS) method applied only to K^+ levels in the vitreous humour, the prediction of PMI with ANN was improved by a factor of 5 from $\approx \pm$ 15 h to less than 3 h.

Keywords Capillary electrophoresis · Forensic science · Artificial neural networks · Post-mortem interval · Vitreous humour

G. Bocaz-Beneventi[1] · J. Havel (✉)
Department of Analytical Chemistry, Faculty of Science,
University of Masaryk, Kotlárská 2, 61137 Brno, Czech Republic
e-mail: havel@chemi.muni.cz, Fax: +420-5-41211214

F. Tagliaro
Institute of Forensic Medicine,
Catholic University of the Sacred Heart, 00168 Rome, Italy

F. Bortolotti · G. Manetto
Department of Public Medicine and Health,
University of Verona, 37134 Verona, Italy

Permanent address:
[1] Department of Laboratories,
Institute of Forensic and Legal Medicine, Ministry of Justice,
Av. La Paz 1012, Santiago, Chile

Introduction

The post-mortem chemical and biochemical analysis of vitreous humour is widely used in modern forensic pathology and forensic toxicology because of the ease of collection and stability after death [1, 2]. The concentrations of sodium, urea and creatinine in the vitreous humour have been used for post-mortem diagnoses of several pathologies (e. g. renal failure, severe dehydration, salt intoxication or excessive water intake) [3, 4, 5]. In addition, the determination of ethanol and drugs in vitreous humour after death is vital for the estimation of drug concentrations present at the time of death and thus to make inferences on the causes of suspected acute intoxication [6, 7].

Another crucial question in forensic science which has been faced by using vitreous humour ion analysis or other methodological strategies, is the determination of the post-mortem time interval [8, 9, 10, 11]. Recently, Tagliaro et al. developed a method for the determination of potassium in human vitreous humour by capillary zone electrophoresis, which was successfully, although preliminarily, applied to the determination of the post-mortem interval [12].

On the another hand, the use of artificial neural networks (ANN) for optimisation of high performance capillary zone electrophoresis (HPCE) methods has gained popularity and has been used with advantage in terms of reduction of the number of experiments, reduced analysis time and enhanced statistical evaluation of data [13, 14, 15, 16, 17, 18, 19].

Although, computerised methods have been used in forensic science with different data sets and for other legal purposes [20, 21, 22, 23, 24, 25, 26, 27, 28, 29], to the best of our knowledge, they have been not applied to the study of ions in vitreous humour to determine the time since death.

The purpose of the present work was to improve the statistical correlation between post-mortem interval and ion concentrations in the human vitreous humor by applying ANN, a computerised chemometrical analysis method.

Artificial neural network theory

The back-propagation network theory

In order to translate how the neural network mimics the human brain into our understanding, the processing of information is divided in three levels. The first level is the input layer which receives the information about the system; the nodes in the input layer are simple distributive nodes, which do not alter the input value at all. The third level is the output layer which is the observable response or behaviour. The second level represents one or more hidden layers, which process the information initiated at the input. The node (neuron) is the basic processing unit in ANN. The node sums the product of each connection weighting (w_{jk}) from the node j to the node k and the input (x_j) and the additional weighting or bias to get the sum value for the node k, Eq. 1:

$$sum_k = \sum_j x_j w_{jk} + \gamma_k \quad (1)$$

where γ is the bias value. The sum_k of the weighted inputs is transformed with a transfer function (mostly sigmoid function) and this function is used to get the output level. We have used a sigmoid function $f(x) = 1/[1/ + \exp(-x/\theta)]$, where x is the weighted sum of inputs and θ is the gain and x is sum_k defined in Eq. 1. The back-propagation network (BPNs) learns by adjusting its weightings according to the error. The goal of the training method is to change the weightings between the layers in a direction that minimises the error (E). The error E of a network, Eq. 2, is defined as:

$$E = \frac{1}{2}\sum_p \sum_j \left(y_{p_j} - t_{p_j}\right)^2 \quad (2)$$

i.e. the squared difference between the target values (desired output) t and the outputs y of the output neurons summed, over p training pattern and j output nodes. The error E is minimised according to the steepest descent method, Eq. 3:

$$\Delta w_{ij}(n) = -\eta \frac{\delta E}{\delta w_{ij}} \quad (3)$$

where η is a positive constant known as the learning rate and $\Delta w_{ij}(n)$ the current weighting change for the weight w_{ij}. The weights are calculated in n-th iteration process.

The gradient descent method can be enhanced by a momentum term from the previous weightings changes as, Eq. 4:

$$\Delta w_{ij}(n) = -\eta \frac{\delta E}{\delta w_{ij}} + \alpha \Delta w_{ij}(n-1) \quad (4)$$

where α (momentum factor) is another constant. The learning rate (*lrate*) controls the update rate according to the new weightings change and the momentum acts as stabiliser being aware of the previous weighting changes. During the training process it is necessary to study the effect of *lrate* and momentum (α) in order to avoid over-fitting problems. The learning process is stopped when the network has reached a proper minimum error.

Materials and methods

Reagents

All chemicals were of analytical reagent grade. Imidazole (99% pure), 18-crown-6-ether (99% pure) and *d*,*l*-alpha-hydroxybutyric acid sodium salt (HIBA) (99% pure) were purchased from Sigma-Aldrich (Steinheim, Germany). Standard solutions of potassium, ammonium, sodium and barium were prepared from AnalaR salts (Merck, Darmstadt, Germany). Water used for sample preparation was of HPLC grade (Carlo Erba, Milan, Italy). The buffer was prepared daily, filtered and degassed under vacuum through a 0.45 μm Prep-Disc teflon filter from Bio-Rad (Hercules, Calif.) prior to use. A Shott Gerate GmbH CG810 pH-meter (Mainz, Germany) was used for the pH measurements.

For experimental details concerning determination of cations in a vitreous humour we refer to the paper reported by Tagliaro et al. [12].

Capillary electrophoresis

A capillary electropherograph P/ACE 5500 (Beckman Coulter, Fullerton, Calif.) with a filter UV absorbance detector, equipped with P/ACE Station (Version 1.0) software was employed for all experiments. An uncoated fused-silica capillary, 75 μm i. d., 47 cm total length and 40 cm length to the detector, was used. Indirect UV absorbance detection was performed at 214 nm.

Electrophoretic separations were carried out in a running buffer containing 5 mM imidazole, 5 mM 18-crown-6-ether and 6 mM *d*,*l*-alpha-hydroxybutyric acid (HIBA) at pH 4.5, the applied voltage was 500 V/cm and the temperature was set at 25 °C. Indirect UV detection was set at 214 nm. The sample solutions were injected hydrodynamically at the anode end of the capillary (0.5 psi for 10 s).

Conditioning of capillary

A new capillary column was conditioned by step-wise rinsing with 1 M NaOH for 10 min, 0.1 M NaOH for 10 min, water for 10 min and running buffer for 20 min. The capillary was washed daily for 5 min with 0.1 M NaOH, for 5 min with water and for 10 min with running buffer. Between each run, the capillary was flushed with 0.1 M NaOH for 2 min, water for 2 min, followed by background electrolyte solution for 6 min. The capillary inlet and outlet vials were replenished after every 10 injections. At the end of the day, the capillary was flushed with 0.1 M NaOH for 1 min and water for 5 min.

Sample collection and preparation

The human vitreous humour samples were obtained from both eyes of 61 cases of authorised autopsies carried out in the Unit of Forensic Medicine, Department of Public Medicine and Health, University of Verona, Verona, Italy. The samples were collected by needle puncture of the posterior chamber of the eye by gentle sucking of about 50 μl of vitreous humour with a 1 ml plastic syringe. All specimens were stored frozen until analysis.

Before injection, vitreous humour samples were diluted 1:20 with a 40 μg/ml aqueous solution of barium as internal standard (I.S.).

Software and data processing

The 61 original data sets corresponding to the response to the detector for peak areas and peak heights of K^+, NH_4^+, Na^+, and Ba^{2+} ions in the vitreous humour were used as input data in an input

layer and post-mortem intervals as an output layer were used for the chemometrical analysis. The software for the ANN method was from the TRAJAN programme (Neural Network Simulator, release 3.0 D, TRAJAN software, 1998), purchased from Trajan Software Ltd. (Trajan House, Co. Durham, UK).

Results and discussion

Figure 1 shows a typical electropherogram of the analysed ions in human vitreous humour samples. For validation data of the method the reader is referred to Tagliaro et al. [12].

PMI estimation using single ion data

The correlation of PMI and vitreous ion concentration was first studied using single ion data and the linear least square regression method (LLS).

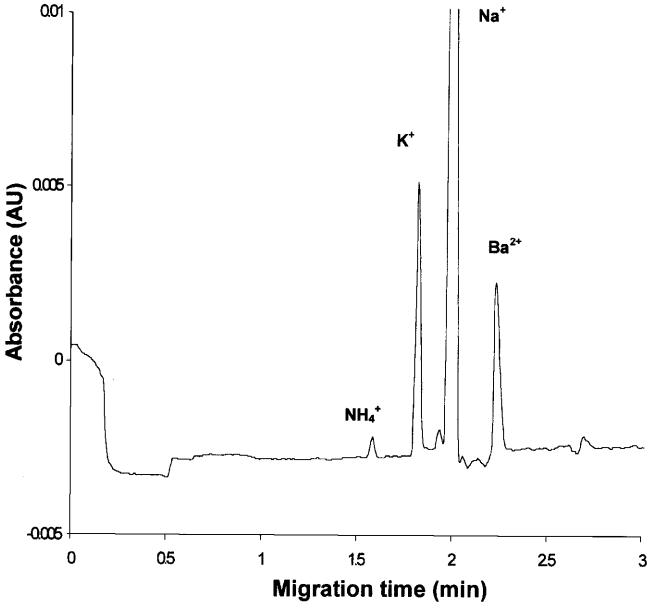

Fig. 1 Example of a CZE electropherogram of cations in human vitreous humour

Figure 2a shows the correlation between PMI and K^+ peak areas, as described by the equation y = 101.1 × –1155.1 (r^2 = 0.8264) (y = peak area; x = PMI) and Fig. 2b the correlation with K^+ peak heights, according to the equation y = 53.1x–1231.2 (r^2 = 0.8920) (y = peak height; x = PMI).

In the case of ammonium ions, the coefficient of correlation was worse than for potassium (r^2 = 0.6625) (Fig. 3), as described by the equation y = 6.9 × –148.2 (r^2 = 0.6625) (y = peak area; x = PMI) and finally Na^+ ions do not show any significant correlation with PMI (r^2 = 0.0407).

Modelling by ANN

In the first stage of evaluation of the potential of ANN, the method was applied to investigate the modelling ability between PMI and available data. Comparison with the values obtained by the conventional LLS approach was done using a data set containing 61 experimental points of PMI vs K^+, Na^+, NH_4^+, and Ba^{2+} (peak height and area). The whole pattern (61 × 9) was processed as the training set on a Pentium personal computer using the back-propagation neural networks method (BPNNs) with the TRAJAN programme. Before any calculations were made the data were normalised by the programme (range 0.1–0.9). First, the optimal structure of ANN was searched. In order to determine the optimal number of nodes in a hidden layer, we plotted the RMS error as a function of the number of neurons in the hidden layer. It is evident from Fig. 4. that 4 or 5 nodes are sufficient to obtain low RMS values and that a further increase in the number of nodes does not bring any improvement. The optimal ANN architecture is shown in Fig. 5.

During the application of BPNN, the goal of net training is to minimise the root mean square error (RMS), Eq. 5:

$$RMS = \sqrt{\frac{\sum_{i=1}^{N}\sum_{j=1}^{M}\left(y_{ij} - out_{ij}\right)^2}{N \times M}} \quad (5)$$

where y_{ij} are the elements of the matrix (N × M) for training or test set, and out_{ij} are the elements of the output matrix (N × M) of the neural network, N is the number of variables in the pattern and M is the number of samples.

Fig. 2 **a** LLS correlation of potassium peak areas with PMI and **b** LLS correlation of potassium peak heights with PMI

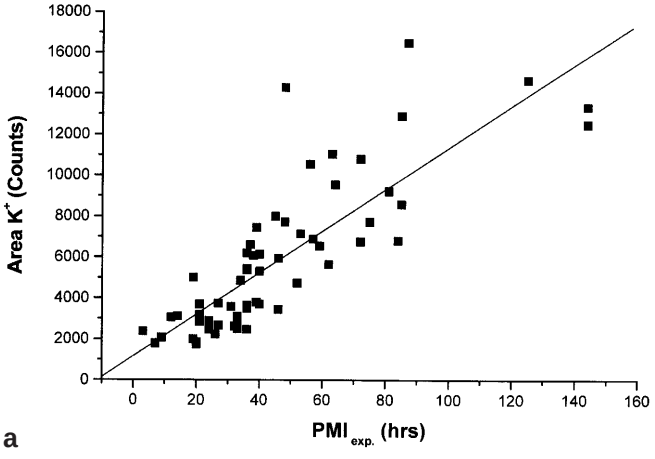

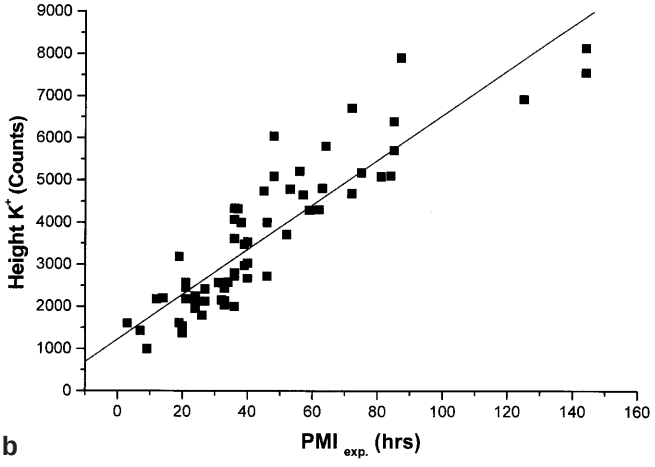

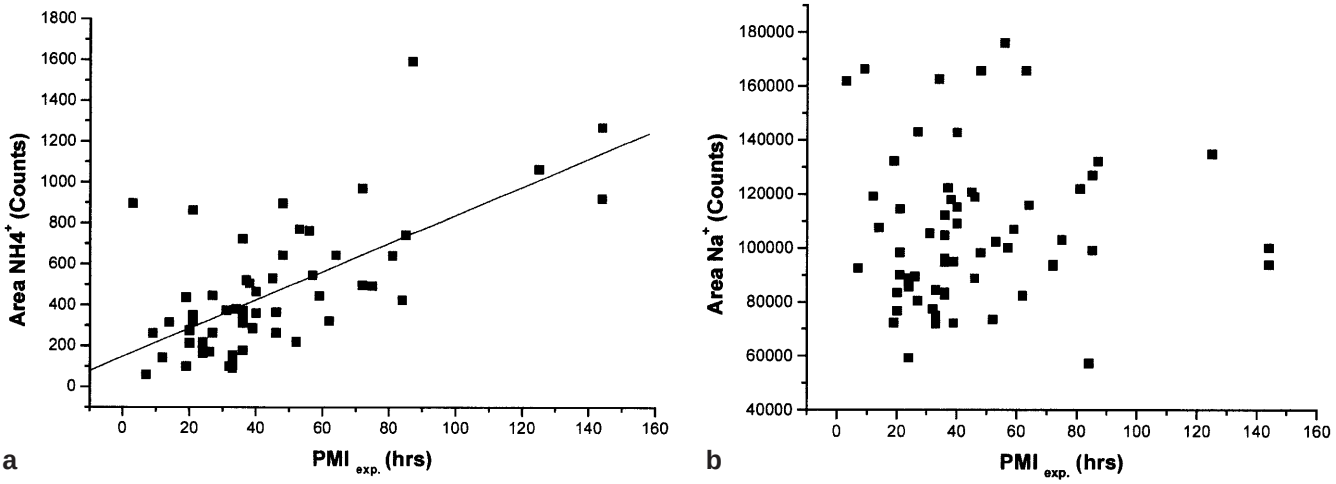

Fig. 3 **a** Correlation of ammonium peak areas with PMI and **b** area of Na^+ peak as a function of PMI

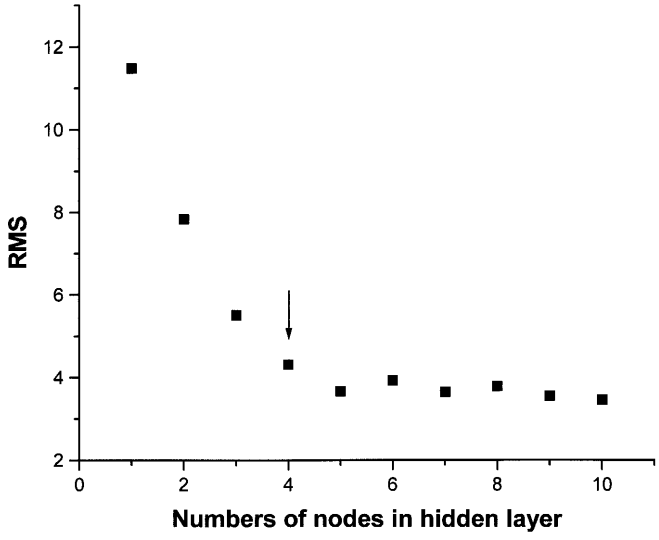

Fig. 4 RMS values versus the number of nodes in the hidden layer

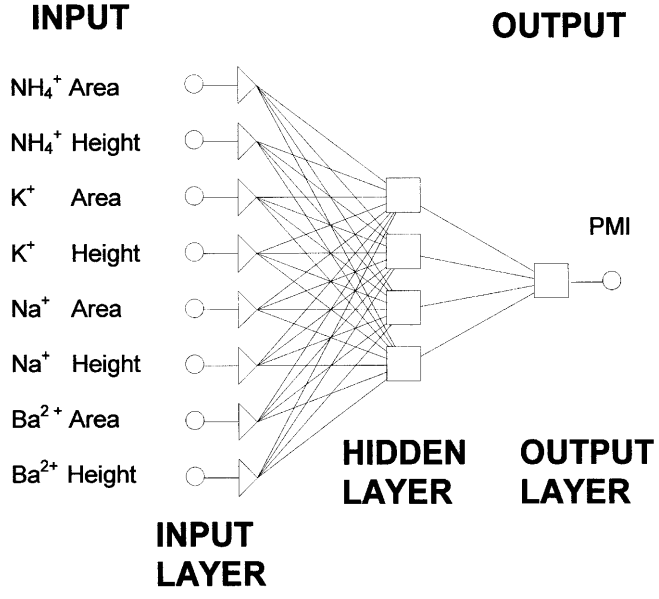

Fig. 5 Optimal ANN structure to model multicomponent analysis of vitreous humour as a function of PMI (8:4:1)

In order to avoid over-training, the performance of the neural network was tested every 100 or 1,000 epochs during the training and the weightings for the minimal RMS (root mean squares Eq. 5) for the learning and test set were recorded. The training conditions were momentum 0.3, learning rate 0.6, as recommended in the Trajan programme (Chapter 3.4). We also tried other values, but those mentioned were optimal. The number of learning cycles was fixed to 40,000. We have stopped the training after this value of epochs was reached as no significant improvement for higher values was obtained. The average value of the error, calculated by Eq. 5, for the complete training set was 5.8% rel. which is an excellent fit, much better than the one obtained using only the K^+ peak area (Fig. 2).

Figure 6 shows the results of modelling applied to the 61 real forensic cases. Excellent correlation between experimental post-mortem interval and PMI values predicted by the ANN was obtained with a coefficient of correlation of 0.9810. Table 1 summarises the estimated values found for PMI using the LLS and ANN models. Significant improvement in the estimation of time after death was obtained when we used the complete available data, as it is shown by the decrease of the error of prediction from 15.28 to 4.69 h (> 3-fold).

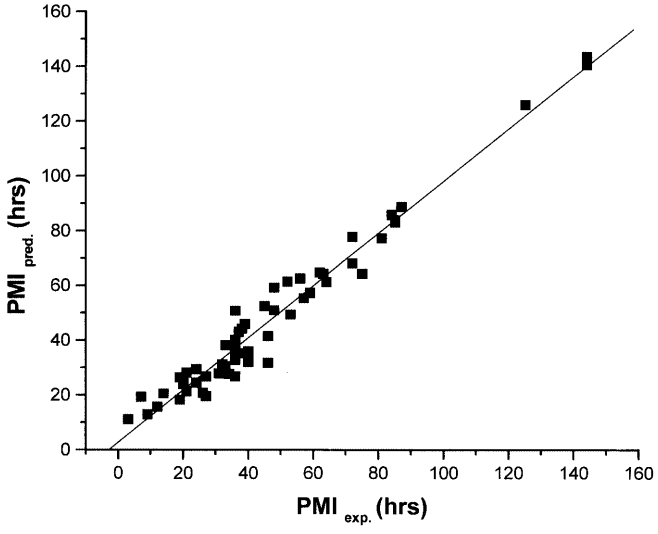

Fig. 6 Correlation of PMI predicted by the multivariate ANN method and the actual PMI

Table 1 Modelling: estimated values of PMI with LLS and ANN using complete data for all cases

Cases	Real PMI (h)	PMI predicted by LLS (h)	Dif. ($PMI_{pred.}$ – $PMI_{exp.}$) (h)	Difference (%)	PMI predicted by ANN (h)	Dif. ($PMI_{pred.}$ – $PMI_{exp.}$) (h)	Difference (%)
1	48.00	129.78	81.78	170.38	50.87	2.87	5.98
2	125.00	133.40	8.40	6.72	125.80	0.80	0.64
3	63.00	97.68	34.68	55.05	64.23	1.23	1.95
4	87.00	151.38	64.38	74.00	88.65	1.65	1.90
5	34.00	36.44	2.44	7.18	27.62	6.38	18.76
6	20.00	5.67	–4.33	71.65	23.99	3.99	19.95
7	40.00	49.27	9.27	23.18	35.57	4.43	11.08
8	36.00	24.47	–1.53	32.03	32.69	3.31	9.19
9	7.00	6.18	–0.82	11.71	19.20	12.20	174.29
10	75.00	64.84	–0.16	13.55	64.20	10.80	14.40
11	40.00	25.12	–14.88	37.20	31.93	8.07	20.18
12	84.00	55.85	–8.15	33.51	85.74	1.74	2.07
13	24.00	14.46	–9.54	39.75	29.38	5.38	22.42
14	19.00	8.13	–10.87	57.21	18.19	0.81	4.26
15	24.00	16.93	–7.07	29.46	29.34	5.34	22.25
16	33.00	13.09	–19.91	60.33	30.52	2.48	7.52
17	33.00	15.03	–17.97	54.45	29.01	3.99	12.09
18	33.00	19.23	–13.77	41.73	38.08	5.08	15.39
19	32.00	14.49	–17.51	54.72	31.16	0.84	2.63
20	52.00	35.32	–16.68	32.08	61.33	9.33	17.94
21	27.00	14.92	–12.08	44.74	26.27	0.73	2.70
22	24.00	12.82	–11.18	46.58	24.50	0.50	2.08
23	36.00	13.04	–22.96	63.78	35.07	0.93	2.58
24	62.00	44.29	–17.71	28.56	64.69	2.69	4.34
25	19.00	37.85	18.85	99.21	26.36	7.36	38.74
26	21.00	19.80	–1.20	5.71	28.05	7.05	33.57
27	36.00	44.22	8.22	22.83	50.71	14.71	40.86
28	46.00	47.47	1.47	3.20	41.47	4.53	9.85
29	85.00	73.34	–11.66	13.72	83.77	1.23	1.45
30	21.00	16.54	–4.46	21.24	21.45	0.45	2.14
31	38.00	48.57	10.57	27.82	44.22	6.22	16.37
32	57.00	56.53	–0.47	0.82	55.20	1.80	3.16
33	48.00	64.83	16.83	35.06	59.17	11.17	23.27
34	72.00	95.34	23.34	32.42	77.72	5.72	7.94
35	14.00	19.24	5.24	37.43	20.53	6.53	46.64
36	40.00	40.99	0.99	2.48	35.87	4.13	10.33
37	59.00	53.18	–5.82	9.86	57.24	1.76	2.98
38	3.00	11.83	8.83	294.33	11.02	8.02	267.33
39	27.00	25.54	–1.46	5.41	19.51	7.49	27.74
40	85.00	116.09	31.09	36.58	83.00	2.00	2.35
41	144.00	111.98	–32.02	22.24	143.50	0.50	0.35
42	36.00	49.86	13.86	38.50	40.13	4.13	11.47
43	53.00	59.12	6.12	11.55	49.32	3.68	6.94
44	31.00	23.82	–7.18	23.16	27.85	3.15	10.16
45	9.00	8.94	–0.06	0.67	12.83	3.83	42.56
46	39.00	62.12	23.12	59.28	45.78	6.78	17.38
47	56.00	92.84	36.84	65.79	62.51	6.51	11.63
48	81.00	79.71	–1.29	1.59	77.21	3.79	4.68
49	20.00	6.64	–13.36	66.80	24.42	4.42	22.10
50	26.00	10.37	–15.63	60.12	20.80	5.20	20.00
51	36.00	12.82	–23.18	64.39	26.73	9.27	25.75
52	46.00	22.56	–23.44	50.96	31.73	14.27	31.02
53	12.00	18.64	6.64	55.33	15.62	3.62	30.17
54	21.00	25.05	4.05	19.29	21.28	0.28	1.33
55	37.00	53.88	16.88	45.62	42.98	5.98	16.16
56	45.00	67.58	22.58	50.18	52.34	7.34	16.31
57	64.00	82.84	18.84	29.44	61.27	2.73	4.27
58	39.00	26.00	–13.00	33.33	35.17	3.83	9.82
59	36.00	41.56	5.56	15.44	38.72	2.72	7.56
60	72.00	55.35	–16.55	23.13	66.88	5.12	7.11
61	144.00	120.56	–23.44	16.28	140.50	3.50	2.43
Sum	–	–	932.31	–	–	286.39	–
Average Residual	–	–	15.28	–	–	4.69	–

Additional calculations

Similar results were obtained when we used only peak areas or peak heights. The number of nodes in the hidden layer was four in both cases. The correlation between the experimental post-mortem interval and PMI values predicted by the ANN using only peak areas, was also satisfactory with an r^2 value of 0.9834. The comparison of PMI values estimated by LLS and ANN shows that the results are slightly worse than those (Table 1) when complete data are used for the calculations. Similarly, using only peak heights the average error of PMI estimate was slightly higher (4.95 h).

The use of barium as internal standard

The changes in the peak heights of Ba^{2+} as the internal standard are due to differences in the amount loaded in the capillary and variation in viscosity of the vitreous humour samples. The presence of a Ba^{2+} peak in the input data acts as a normalisation factor in the neural network calculations. Without this information the average residuals of modelling and prediction were greater than those when complete data sets were used. While average residuals for modelling and prediction of complete data were 4.69 and 2.83, without Ba^{2+} the values obtained were 4.80 and 4.05, respectively.

Also, the normalisation procedure of all data (areas and heights) using peak heights for barium was made but the estimation of PMI using this approach does not improve the precision of modelling and prediction.

Prediction by ANN

The data set was divided into the learning set (51 patterns) and the test set (10 patterns). Good agreement between PMI_{exp} and PMI_{pred} by the ANN method for the complete training set was observed when we used either all available data, peak areas or heights. Then, in order to check the proposed method, data sets corresponding to 10 selected forensic cases, not included in the training set, were tested. The comparison of both methodologies of prediction was done. Table 2 shows the results of the prediction obtained by LLS (for K^+ only) and by the ANN method using all available data, peak areas and peak heights, respectively. PMI values predicted by ANN were in all cases much better (more than 3 times) than the values obtained by the classical LLS method. Using only peak areas or peak heights the difference in the average residual was not significant. However, the best prediction of PMI (5.2 times) was achieved using all available data.

The results show for the first time the usefulness of multivariate data ion analysis in the vitreous humour by CZE-ANN for inferring on the time since death. In particular, ANN modelling and prediction to estimate the post-mortem interval proved to be much more accurate than the LLS method conventionally used for this purpose.

In conclusion, in the present work ANN was used for the first time to model correlation between vitreous humour cation analysis and PMI with a very good fit. To this aim CZE, which provides direct, accurate and simultaneous determination of potassium, ammonium, sodium, barium in untreated vitreous humour, offers an almost ideal instrumental tool.

In comparison to the traditional approach based on a linear correlation between potassium concentration and

Table 2 Prediction of PMI values for 10 selected forensic cases: comparison of conventional LLS and proposed ANN methods

Cases	Real PMI (h)	PMI predicted by LLS (h)	Difference (PMI_r–PMI_e) (h)	PMI predicted by ANN All data (h)	Difference (PMI_r–PMI_e) (h)	PMI predicted by ANN Peak areas (h)	Difference (PMI_r–PM_e) (h)	PMI predicted by ANN Peak heights (h)	Difference (PMI_r–PMI_e) (h)
6	20.00	5.67	–14.33	23.17	3.17	23.68	3.68	11.59	–8.41
12	84.00	55.85	–28.15	84.33	0.83	88.55	4.55	80.10	–3.90
19	32.00	14.49	–17.51	31.14	–0.86	30.99	1.01	30.89	–1.11
21	27.00	14.92	–12.08	25.58	–1.42	31.04	4.04	29.46	2.46
29	85.00	73.34	–11.66	77.92	–7.08	84.98	0.02	80.21	–4.79
32	57.00	56.53	–0.47	54.39	–2.61	57.30	0.30	52.62	–4.38
41	144.00	111.98	–32.02	143.50	–0.50	98.93	45.07	132.30	–11.70
44	31.00	23.82	–7.18	29.00	–2.00	30.85	0.15	32.27	1.27
54	21.00	25.05	4.05	24.02	3.02	23.66	2.66	33.20	12.20
57	64.00	82.84	18.84	57.23	–6.77	63.80	0.20	64.27	0.27
Sum	–	–	146.29	–	28.26	–	61.68	–	50.49
Average Residual	–	–	14.63	–	2.83, 3.04[a]	–	6.17	–	5.05

[a] In the course of the revision of the manuscript additional cases were collected. From a total of 72 cases the average difference in prediction was 3.04 h

post-mortem time, the proposed model greatly improves the prediction of the post-mortem interval.

These considerations are particularly relevant if we consider that vitreous humour ion analysis is in practice the only objective tool to infer on the time of death in the hands of forensic pathologists in the time window 1–5 days after death (when the body temperature has reached the ambient temperature).

On the basis of these considerations, multivariate analysis of different parameters which can easily been performed by ANN seems to be the best strategy to infer on the time of death, also in respect to the general rules of admissibility in court.

Acknowledgements G. Bocaz-Beneventi would like to thank to the Government of the Republic of Chile and the authorities of the Institute of Forensic and Legal Medicine of Chile for the support for his Ph.D. studies at Masaryk University. This work was partly supported by the Ministry of Education and Youth of the Czech Republic, grant No. CEZ: J 07/98: 143100011. From the Italian side, funding was obtained from research grants awarded by Regione Veneto (# 765/01/97), CARIVERONA and M.U.R.S.T. (# 9906404127).

References

1. Coe JI (1989) Vitreous potassium as a measure of the post-mortem interval: an historical review and critical evaluation. Forensic Sci Int 42:201–213
2. Coe JI (1993) Postmortem chemistry update. Emphasis on forensic applications. Am J Forensic Med Pathol 14:91–117
3. Huser CJ, Smialek JE (1986) Diagnosis of sudden death in infants due to acute dehydration. Am J Forensic Med Pathol 7: 278–282
4. Carlson JA, Middleton PJ, Szmanski MT, Huber J, Petric M (1978) Fatal rotavirus gastroenteritis: an analysis of 21 cases. Am J Dis Child 132:477–479
5. Vieweg WV, David JJ, Rowe WT, Wampler GJ, Burns WJ, Spradlin WW (1985) Death from self-induced water intoxication among patients with schizophrenic disorders. J Nerv Ment Dis 173:161–165
6. McKinney PE, Phillips S, Gomez HF, Brent J, MacIntyre M, Watson WA (1995) Vitreous humor cocaine and metabolite concentrations: do postmortem specimens reflect blood levels at the time of death? J Forensic Sci 40:102–107
7. Logan BK, Stafford DT (1990) High-performance liquid chromatography with column switching for the determination of cocaine and benzoylecgonine concentrations in vitreous humor. J Forensic Sci 35:1303–1309
8. Madea B, Henssge C, Honig W, Gerbracht A (1989) References for determining the time of death by potassium in vitreous humor. Forensic Sci Int 40:231–243
9. James RA, Hoadley PA, Sampson B (1997) Determination of postmortem interval by sampling vitreous humour. Am J Forensic Med Pathol 18:158–162
10. Henssge C, Althaus L, Bolt J, Freislederer A, Haffner H-T, Henssge CA, Hoppe B, Schneider V (2000) Experiences with a compound method for estimating the time since death I. Rectal temperature nomogram for time since death. Int J Legal Med 113:303–319
11. Henssge C, Althaus L, Bolt J, Freislederer A, Haffner H-T, Henssge CA, Hoppe B, Schneider V (2000) Experiences with a compound method for estimating the time since death II. Integration of non-temperature-based methods. Int J Legal Med 113:320–331
12. Tagliaro F, Manetto G, Cittadini F, Marchetti D, Bortolotti F, Marigo M (1999) Capillary zone electrophoresis of potassium in human vitreous humour: validation of a new method. J Chromatogr B Biomed Sci Appl 733:273–279
13. Havel J, Peña-Méndez EM, Rojas-Hernández A, Doucet J-P, Panaye A (1998) Neural networks for optimization of high-performance capillary zone electrophoresis methods. A new method using a combination of experimental design and artificial neural networks. J Chromatogr A 793:317–329
14. Farková M, Peña-Méndez EM, Havel J (1999) Use of artificial neural networks in capillary zone elctrophoresis. J Chromatogr A 848:365–374
15. Dohnal V, Farková M, Havel J (1999) Prediction of chiral separations using a combination of experimental design and artificial neural networks. Chirality 11:616–621
16. Pokorná L, Revilla AL, Havel J, Patočka J (1999) Capillary zone electrophoresis determination of galanthamine in biological fluids and pharmaceutical preparatives: experimental design and artificial neural network optimization. Electrophoresis 20:1993–1997
17. Havel J, Madden JE, Haddad PR (1999a) Prediction of retention time for anions in ion chromatography using artificial neural networks. Chromatographia 49:481–488
18. Havel J, Breadmore M, Macka M, Haddad PR (1999b) Artificial neural networks for computer-aided modelling and optimization in micellar electrokinetic chromatography. J Chromatogr A 850: 345–353
19. Madden JE, Avdalovic N, Haddad PR, Havel J (2000) Prediction of retention times for anions in linear gradient elution ion chromatography with hydroxide eluents using artificial neural networks. J Chromatogr A 910:173–179
20. Casale JF, Watterson JW (1993) A computerized neural network method for pattern recognition of cocaine signatures. J Forensic Sci 38:292–301
21. Kingston C (1992) Neural networks in forensic science. J Forensic Sci 37:252–264
22. Schoenly K, Goff ML, Early M (1992) A basic algorithm for calculating the post-mortem interval from arthropod successional data. J Forensic Sci 37:808–823
23. Williams AB, Friedman RB, Lorton L (1989) A new algorithm for use in computer identification. J Forensic Sci 34:682–686
24. Lorton L, Rethman M, Friedman R (1988) The computer-assisted postmortem identification (CAMPI) system: a computer-based identification program. J Forensic Sci 33:977–984
25. Cox RJ, Mitchell SL, Espinoza EO (1994) CompuTOD, a computer program to estimate time of death of deer. J Forensic Sci 39:1287–1299
26. Spiehler VR (1989) Computer-assisted interpretation in forensic toxicology: morphine involved death. J Forensic Sci 34: 1104–1115
27. Karlsson T (1999) Multivariate analysis (“forensiometrics”) – a new tool in forensic medicine. Findings on the victim of sharp-force homicide can predict the inter-relationship with the perpetrator. Forensic Sci Int 101:33–41
28. Karlsson T (1999) Multivariate analysis (“forensiometrics”) – a new tool in forensic medicine. Differentiation between firearm-related homicides and suicides. Forensic Sci Int 101:131–140
29. Lynnerup N (1993) A computer program for estimation of time since death. J Forensic Sci 38:816–820